



## Structural Design of the DTU-ESA MM-Wave Validation Standard Antenna

**Branner, Kim; Berring, Peter; Markussen, Christen Malte; Kim, Oleksiy S.; Jørgensen, R.; Pivnenko, Sergey; Breinbjerg, Olav**

*Published in:*  
Proceedings of the 20th International Conference on Composite Materials

*Publication date:*  
2015

*Document Version*  
Publisher's PDF, also known as Version of record

[Link back to DTU Orbit](#)

*Citation (APA):*  
Branner, K., Berring, P., Markussen, C. M., Kim, O. S., Jørgensen, R., Pivnenko, S., & Breinbjerg, O. (2015). Structural Design of the DTU-ESA MM-Wave Validation Standard Antenna. In *Proceedings of the 20th International Conference on Composite Materials ICCM20* Secretariat.

---

### General rights

Copyright and moral rights for the publications made accessible in the public portal are retained by the authors and/or other copyright owners and it is a condition of accessing publications that users recognise and abide by the legal requirements associated with these rights.

- Users may download and print one copy of any publication from the public portal for the purpose of private study or research.
- You may not further distribute the material or use it for any profit-making activity or commercial gain
- You may freely distribute the URL identifying the publication in the public portal

If you believe that this document breaches copyright please contact us providing details, and we will remove access to the work immediately and investigate your claim.

## STRUCTURAL DESIGN OF THE DTU-ESA MM-WAVE VALIDATION STANDARD ANTENNA

K. Branner<sup>1</sup>, P. Berring<sup>1</sup>, C.M. Markussen<sup>1</sup>, O.S. Kim<sup>2</sup>, R. Jørgensen<sup>3</sup>, S. Pivnenko<sup>2</sup> and O. Breinbjerg<sup>2</sup>

<sup>1</sup>Department of Wind Energy, Technical University of Denmark  
P.O. Box 49, Frederiksborgvej 399, DK-4000 Roskilde, Denmark  
Email: [kibr@dtu.dk](mailto:kibr@dtu.dk), web page: [http:// www.vindenergi.dtu.dk](http://www.vindenergi.dtu.dk)

<sup>2</sup>Department of Electrical Engineering, Technical University of Denmark  
Ørstedes Plads, Building 348, DK-2800 Kgs. Lyngby, Denmark  
Email: [osk@elektro.dtu.dk](mailto:osk@elektro.dtu.dk), web page: [http:// www.elektro.dtu.dk](http://www.elektro.dtu.dk)

<sup>3</sup>TICRA, Læderstræde 34, DK-1201 Copenhagen, Denmark  
Email: [rj@ticra.com](mailto:rj@ticra.com), web page: [http:// www.ticra.com](http://www.ticra.com)

**Keywords:** Structural design, Antenna, CFRP, Thermally stable, Mechanically stable, Finite element analysis

### ABSTRACT

A new specially designed antenna to be used for inter-comparisons and validation of antenna test facilities is under development in cooperation between DTU and TICRA under a contract from the European Space Agency.

The antenna is designed to be extremely thermally and mechanically stable in the range of temperatures  $20\pm 5^{\circ}\text{C}$  under arbitrary orientation in the gravity field. The antenna has a characteristic length of approximately 500mm. And in order to obtain very low measuring error, the allowable deformations of the reflector and feeds are down to  $2.5\mu\text{m}$ .

The antenna is modelled structurally using the commercial finite element package MSC.Patran with MSC.MARC as solver. The solid parts of the antenna are meshed with 10-noded tetrahedral elements, which have quadratic shape functions and the entire model has approximately 325.000 elements. The individual solid part of the antenna is connected via a glued contact formulation in MSC.MARC. Because of the size and the complexity of the model a computer cluster is applied to solve the analyses.

This paper describes the structural solution to meet these extremely strict stability requirements and the structural analyses done in order to verify that they can be met. The paper also discusses the challenges of integrating an aluminum feed cluster with high thermal expansion coefficient in a CFRP support frame with very low thermal expansion coefficient.

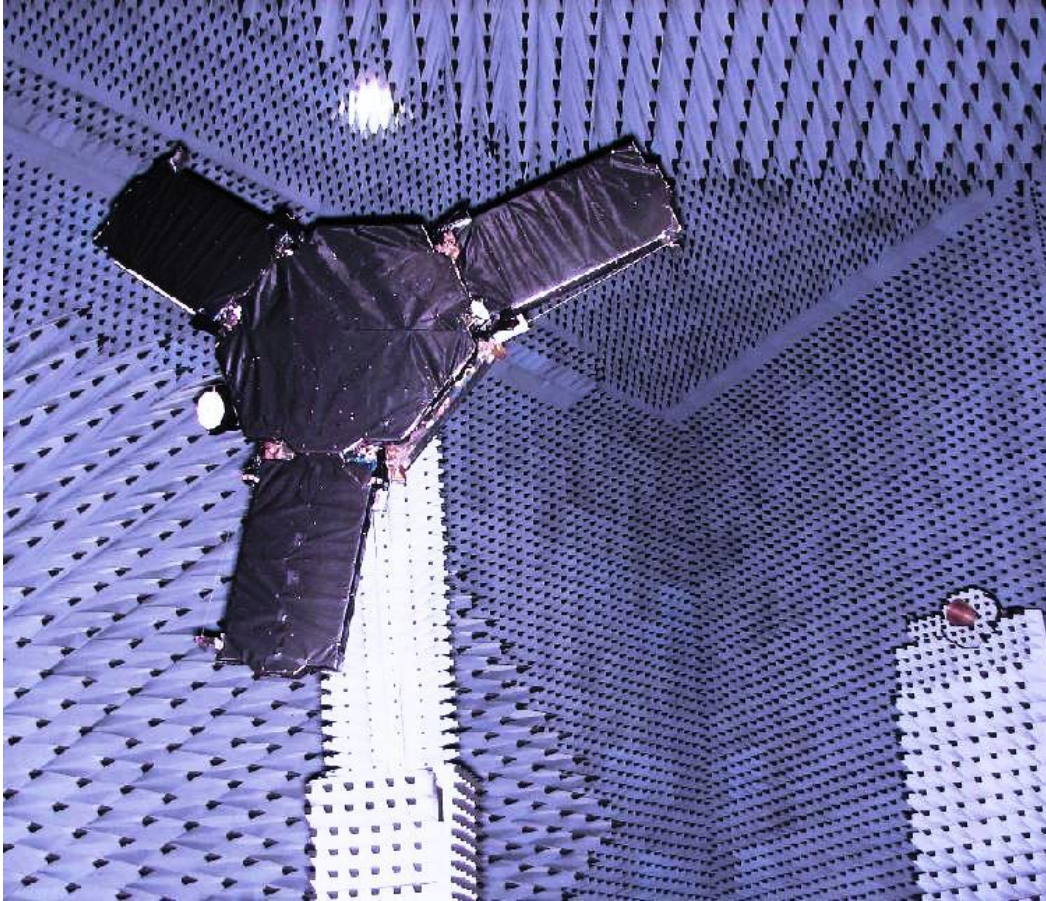


Figure 1: Radiation tests of the central part of the MIRAS radiometer for ESA's SMOS mission in the Radio Anechoic Chamber at DTU Electrical Engineering and part of the DTU-ESA Spherical Near-Field Antenna Test Facility [1].

## 1 INTRODUCTION

Antenna measurements are important for design validation and for demonstration of the performance of the manufactured antennas used in space as well as on earth. Such antenna measurements are often made at indoor measurement facilities equipped with a so called anechoic chamber. That is a room designed to completely absorb reflections of electromagnetic waves (see Figure 1).

In order to make sure that different antenna measurement facilities provide similar measurement results of high quality, specially designed and manufactured Validation Standard (VAST) antennas are used for this purpose [2]. A VAST antenna shall be designed stiff enough such that any deformities of the antenna during test, introduce an error much less than the measurement accuracy being sought. In this case the target is that the introduced error is 10 times less than the measurement accuracy. Therefore, driving requirements to VAST antennas are their mechanical stability with respect to any orientation of the antenna in the gravity field and thermal stability over a given operational temperature range. See more in [3] and [4].

A multi-band millimeter-wave VAST (mm-VAST) antenna has been designed in collaboration between the Technical University of Denmark (DTU) and TICRA under contract from the European Space Agency (ESA). These millimeter-wave bands, 20GHz – 50GHz, are currently being taken into use for space and mobile telecommunication applications. The mm-VAST antenna has passed the critical design review at ESA and has now been manufactured at DTU.

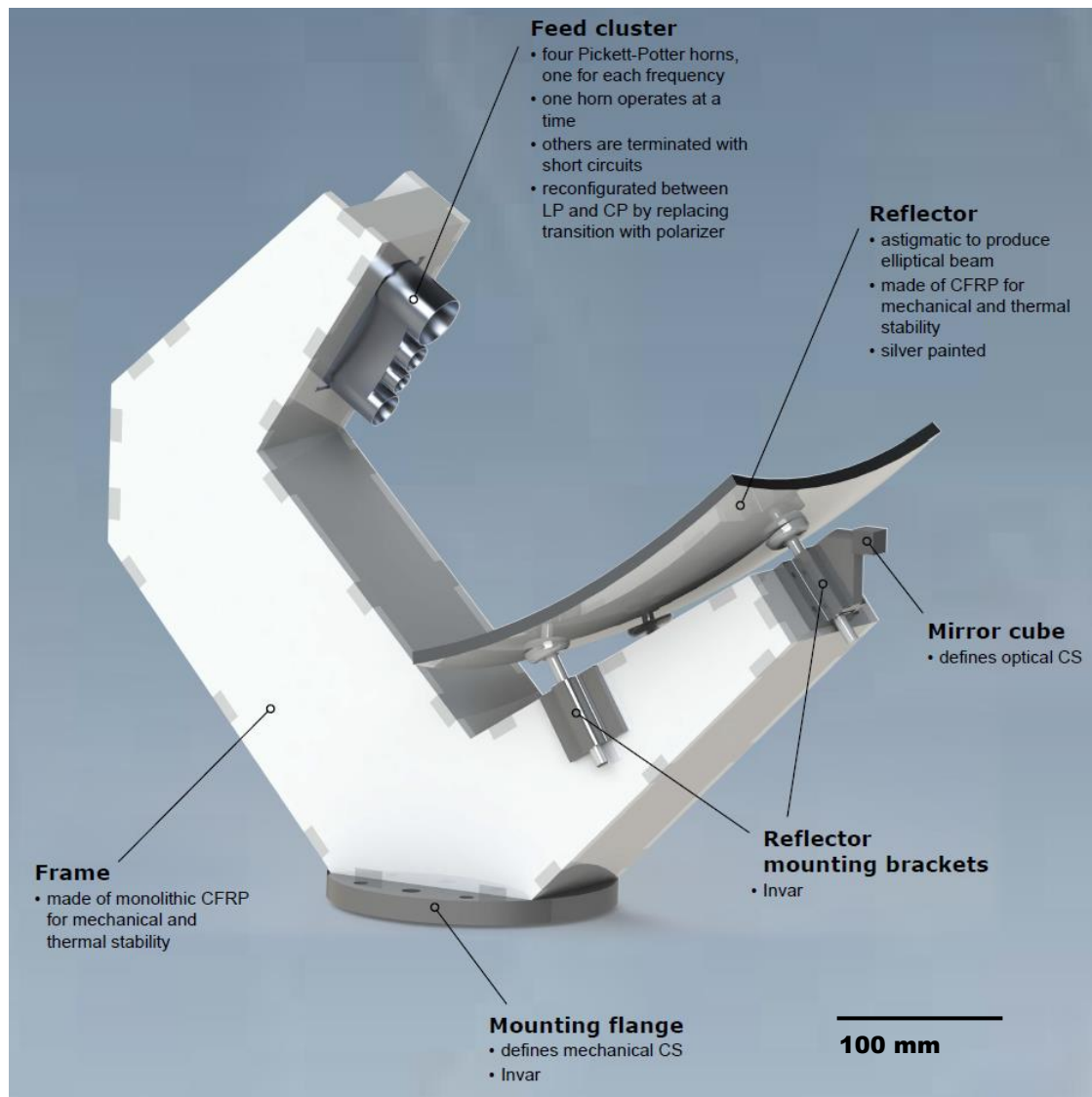


Figure 2: The DTU-ESA Millimeter-Wave Validation Standard Antenna (mm-VAST).

## 2 SUPPORT FRAME DESIGN

A plot of the 3D model is shown in Figure 2. The support frame and reflector are made of 8mm thick carbon fiber reinforced plastic (CFRP) panels. The feed cluster mounting interface, the antenna mounting flange and reflector mounting pins and brackets are made in Invar. These materials are chosen in order to provide the optimum combination of mechanical strength and thermal stability, as they have very low thermal expansion coefficient and high stiffness. The Invar parts are bonded to the CFRP parts by an epoxy adhesive.

## 3. STRUCTURAL FINITE ELEMENT MODEL

This section covers the description of the Finite Element Modelling (FEM) of the antenna and the numerical investigations of the response of the antenna when subjected to a number of different load cases.

### 3.1 Software and model applied in the numerical investigations

The antenna was modelled using the commercial finite element package MSC.Patran (version 2012.2) and MSC.MARC was applied as solver in all analyses.

A detailed solid CAD model was created in Pro/ENGINEER consisting of the main parts of the antenna. A simplified version of this solid CAD model was then imported into MSC.Patran via the STEP file format. The simplification of the CAD model, used as input data for the FE-model, consisted of a clean-up of some of the geometry, such as removing small holes, chambers and rounding which do not have an effect on the overall structural response. Furthermore, bolts, washers, etc. were excluded from the model.

The FE-model of the antenna consists of the following parts/groups:

- Main frame
- Mounting flange
- Mounting frame for the feed cluster
- Feed cluster
- Reflector
- Mounting system for reflector

All of the solid parts are meshed with 10-noded tetrahedral elements which have quadratic shape functions. The entire model has approximately 325.000 elements and all parts have two or more elements through the thickness. The individual solid part of the antenna is connected via MSC.MARC's glued contact formulation. Because of the size and the complexity of the model a computer cluster is used to obtain solutions within reasonable time.

### 3.2 Material model applied in the analysis

All materials are assumed to be linear elastic and isotropic.

The real support frame and reflector consists of a carbon fibre reinforced plastic (CFRP) quasi-isotropic layup which has isotropic-like properties in-plane while the out-of-plane properties are dominated by the resin. As the support frame panels and the reflector are thin walled structures the out-of-plane properties of the CFRP layup is assumed to be negligible and a 3D isotropic material model is therefore applied for these two parts.

The mounting system for the reflector, which consists of the brackets and the pins applied to mount the reflector, is modeled as one part applying the Invar36 material model. This material is also used for the feed cluster mounting interface and for the antenna mounting flange.

The aluminum material model is applied for feed cluster. The material models used in the numerical investigations are presented below in Table 1.

Material model	CFRP iso	Invar36	Aluminum
E [GPa]	55	141	70
$\nu$	0.3	0.3	0.3
$\alpha$ [ $10^{-6}$ m/(m K)]	2.1	1.0	23
$\rho$ [kg/m <sup>3</sup> ]	1920	9600	2700
Note:	The density in this table is multiplied with a factor of 1.2	The density in this table is multiplied with a factor of 1.2	

Table 1: Material models.



Some parts are not modelled directly in the FE-model but are taken into account as additional masses. The additional masses are as follows:

1. Measuring equipment mounted to back side of feed cluster, 4 alternatives
  - a. Horn 1 (largest, top): 200g, COG ( $x_f, y_f, z_f$ )=(48.5mm,0,-128mm)
  - b. Horn 3: 150g, COG ( $x_f, y_f, z_f$ )=(19mm,0,-120mm)
  - c. Horn 4 (smallest): 650g, COG ( $x_f, y_f, z_f$ )=(0,0,-190mm)
  - d. Horn 2 (bottom): 150g, COG ( $x_f, y_f, z_f$ )=(-22mm,0,-120mm)
2. Box mounted to the feed cluster support arm, dimensions: 100x150x40 mm, 500g
3. Shield plate mounted to the support frame, CFRP plate 4mm thick, 300g
4. Level mounted to the side of the support frame, 250g
5. Mirror cube and its cover mounted to the reflector support arm
6. Other mass: adhesive, filler, paint, screws etc., 7%

The 4 horns in the feed cluster are seen in Figure 2. Of the 4 alternatives (item 1) the measuring equipment mounted to back side of feed cluster, horn 4 is the worst from a loading point of view and are modelled as a point mass at its center of gravity and connected to the feed cluster horn 4 by a rigid beam. The center of gravity and defined in the feed cluster coordinate system as shown in Figure 3.

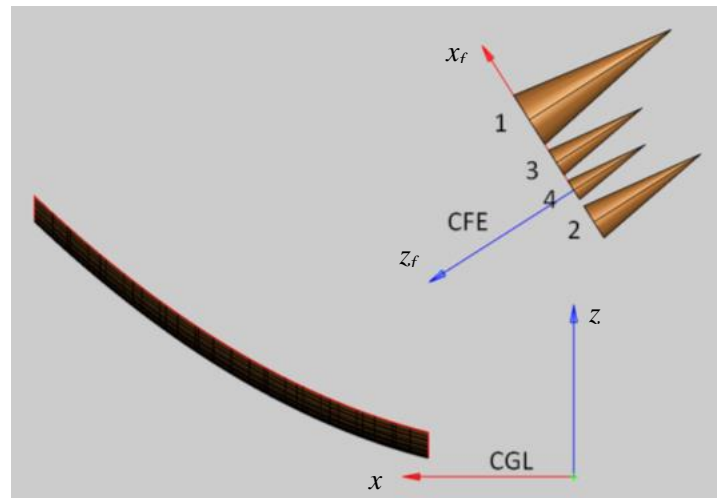


Figure 3: Definition of the global coordinate system (CGL) and feed cluster coordinate system (CFE) with origin in center of horn 4.

The other items 2-6 are modelled as mass spread out over the FE-model. According to the CAD model the mass of frame with reflector, Invar36 mounting flange and Invar36 feed interface is 8402g. The mass of the aluminum feed cluster is 754g. Item 2-5 have a total mass of 1100g which corresponds to 13% of the 8402g. The remaining mass (item 6) is assumed to correspond to 7% of the 8402g. Therefore, the additional mass to be spread out over the structure is 20% corresponding to a density increase of 20% for the invar and CFRP materials.

### 3.3 Analysis preformed in FEA

In the simulations the nodes associated with the bottom surfaces of the mounting flange is fully fixed. It is assumed, and also verified by the analyses, that response of the antenna is linear and therefore is superposition of the computed displacements and rotations valid. Four different load configurations are performed numerically:

1. A thermal load case of a temperature change of 500°C
2. A gravity load of 981m/s<sup>2</sup> in x-direction with respect to the global coordinate system
3. A gravity load of 981m/s<sup>2</sup> in y-direction with respect to the global coordinate system
4. A gravity load of 981m/s<sup>2</sup> in z-direction with respect to the global coordinate system

The numerical loads configurations are scaled with a factor of 100 compared with the design load cases. In a sensitivity study it was found that the numerical results were affected by uncertainties as the displacements response of the antenna model, when subjected to the design load cases were too small to compute with an acceptable precision in the numerical setup.

In Figures 4-7 the deformation of the antenna predicted by FEA are shown for the four different numerical load configurations.

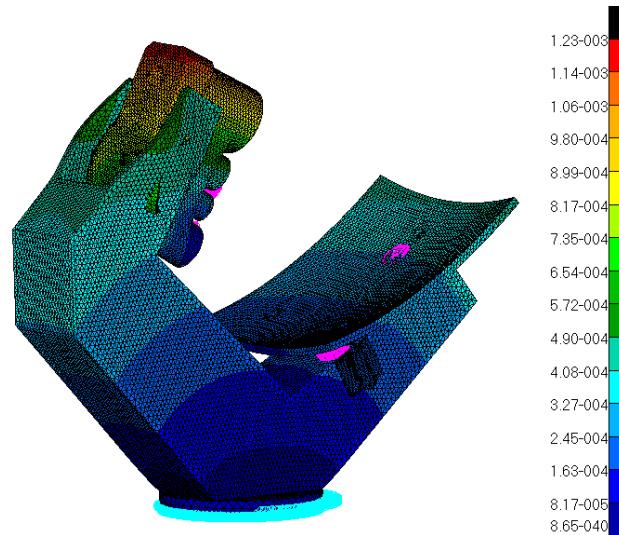


Figure 4: The deformed results of the thermal load case (temperature change of 500°C). Plot of the magnitude displacements [m], visual scaling factor is 100.

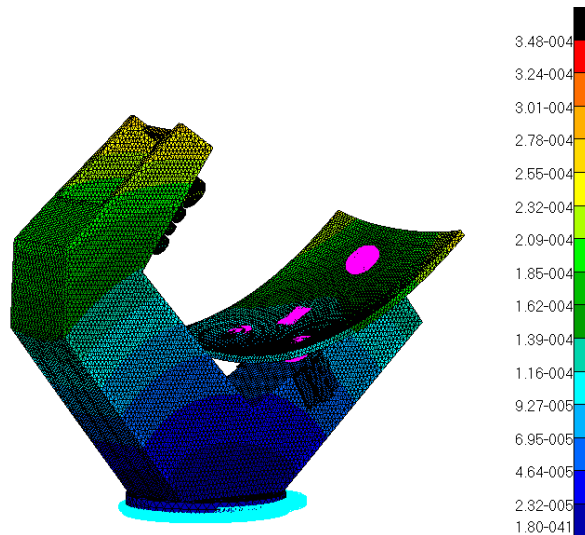


Figure 5: The deformed results of gravity in global x-axis load case ( $g_x = 981\text{m/s}^2$ ). Plot of the magnitude displacements [m], visual scaling factor is 100.

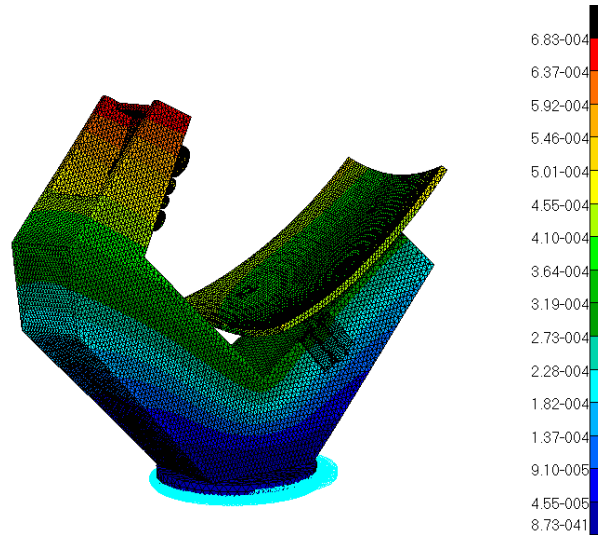


Figure 6: The deformed results of gravity in global y-axis load case ( $g_y = 981\text{m/s}^2$ ). Plot of the magnitude displacements [m], visual scaling factor is 100.

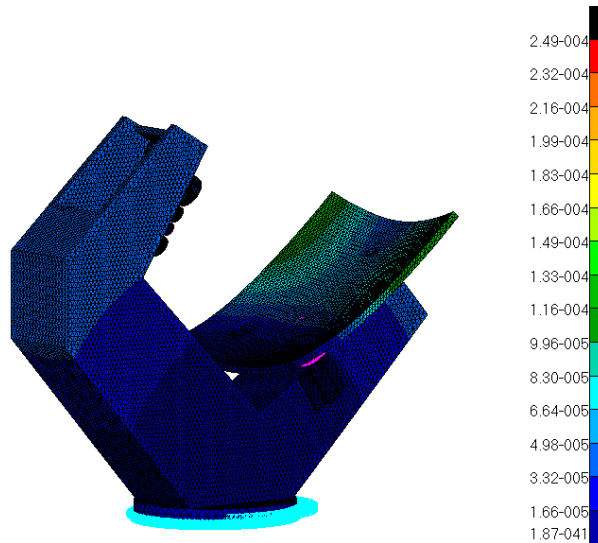


Figure 7: The deformed results of gravity in global z-axis load case ( $g_z = 981\text{m/s}^2$ ). Plot of the magnitude displacements [m], visual scaling factor is 100.

### 3.4 Challenge of integrating the aluminum feed cluster

The feed cluster is made of aluminum, which has a thermal expansion coefficient of approximately  $23 \times 10^{-6} \text{ m/(m K)}$ , which is relative high in this context. And which is approximately 10 times higher than the thermal expansion coefficient for the CFRP layup and approximately 20 times higher than for Invar36.

As it can be seen in Figure 4, the feed cluster also expands much more to temperature increase than the rest of the structure. In order to minimize the deformations of the CFRP structure introduced by the thermal expansion of the aluminum feed cluster, an air gap is made around the feed cluster as shown in Figure 8. Furthermore, the feed cluster is mounted on an Invar36 frame, which then is glue to the CFRP support frame. The feed cluster is bolted the Invar36 interface with 4 bolts around horn 4, where the stability tolerance requirements are most strict. This enables the ends of the feed cluster to expand freely as seen in Figure 8. As the distance between the feed cluster and the reflector needs to be very stable during operation, the design is made so the thermal expansion or contraction of the



aluminum feed cluster compensates partly for the increase or decrease in distance between the feed cluster and the reflector due to thermal expansion or contraction of the CFRP support frame.



Figure 8: Design of the feed cluster interface with the CFRP structure.

#### 4 MECHANICAL AND THERMAL ANALYSES RESULTS

The antenna is designed to be extremely thermally and mechanically stable in the range of temperatures  $20 \pm 5^\circ\text{C}$  under arbitrary orientation in the gravity field. By electromagnetic analyses TICRA calculated the acceptable deformations of the antenna during measurements in order to obtain the required very low effect on the measurement error for the validation antenna. The allowable deformations of the reflector and feeds are here compared with the results from the FEA.

The numerical simulations are done for the following load cases:

1. Deflection due to temperature change alone,  $\pm 5^\circ\text{C}$ .
2. Deflection due to gravity direction, steps of 10 deg. around the x-axis.
3. Deflection due to gravity direction, steps of 10 deg. around the y-axis.
4. Deflection due to gravity direction, steps of 10 deg. around the z-axis.

As the resulting deformations are very small the deformations can be added by superposition in order to compute the response of the combined design load cases.

In order to compute the mechanical and thermal stability of the design focus is kept on the deformation of the feed cluster and reflector. The displacements and rotations of the four feed horn holes and the focal point of the reflector are computed via Multi Point Constrain MPC elements of the type RBE3 which is a linear interpolations element. This type of element does not constrain the nodes applied to compute the displacements and rotations. The four MPC elements applied to compute the displacements and rotations of the feed horn holes have a master node located at the center of holes and this node is coupled to the nodes in the periphery of the hole.

A number of nodes on the reflector close to the focal point are selected to calculate the translation and rotation of the reflector using the least squares method. The MPC elements applied to compute the displacements and rotations of the reflector consist of a master node located in the focal point of the reflector which is coupled to the nodes on the top surfaces of the reflector in an area of approximately  $40 \times 40 \text{ mm}$ .

The deformation of the 4 corners of the reflector is used to calculate the deformation of the reflector.

In Table 2 and 3 the maximum deformations for horn 4 and 1 relative to the reflector are listed and compared with the TICRA requirements. The deformations are calculated in the feed cluster coordinate system. The rotation of the reflector is counted twice in order to account for both the angle of incidence and reflection.

		TICRA analysis	FEM results max deformation
1.1	Movement of feed cluster in $x_f$ direction	$\pm 5 \mu\text{m}$	$0.4 \mu\text{m}$
1.2	Movement of feed cluster in $y_f$ direction	$\pm 5 \mu\text{m}$	$0.9 \mu\text{m}$
1.3	Movement of feed cluster in $z_f$ direction	$\pm 5 \mu\text{m}$	$1.5 \mu\text{m}$
1.4	Rotation of feed cluster around $x_f$ axis	$0.033^\circ$	$0.0010^\circ$
1.5	Rotation of feed cluster around $y_f$ axis	$0.038^\circ$	$0.0020^\circ$
1.6	Rotation of feed cluster around $z_f$ axis	$0.2^\circ$	$0.0003^\circ$

Table 2: Gravitation/temperature stability tolerances for feed cluster, horn 4.

		TICRA analysis	FEM results max deformation
1.1	Movement of feed cluster in $x_f$ direction	$\pm 10 \mu\text{m}$	$6.1 \mu\text{m}$
1.2	Movement of feed cluster in $y_f$ direction	$\pm 10 \mu\text{m}$	$1.6 \mu\text{m}$
1.3	Movement of feed cluster in $z_f$ direction	$\pm 10 \mu\text{m}$	$2.9 \mu\text{m}$
1.4	Rotation of feed cluster around $x_f$ axis	$0.025^\circ$	$0.0010^\circ$
1.5	Rotation of feed cluster around $y_f$ axis	$0.025^\circ$	$0.0024^\circ$
1.6	Rotation of feed cluster around $z_f$ axis	$0.2^\circ$	$0.0003^\circ$

Table 3: Gravitation/temperature stability tolerances for feed cluster, horn 1.

In Table 4 the maximum deformations of the reflector are listed and compared with the TICRA requirements in the global coordinate system. The rotations in 2.4 and 2.5 slightly exceed the requirements, but are deemed acceptable.

		TICRA analysis	FEM results max deformation
2.1	Movement of reflector in x direction	$\pm 5 \mu\text{m}$	$3.0 \mu\text{m}$
2.2	Movement of reflector in y direction	$\pm 5 \mu\text{m}$	$3.6 \mu\text{m}$
2.3	Movement of reflector in z direction	$\pm 2.5 \mu\text{m}$	$2.0 \mu\text{m}$
2.4	Rotation of reflector around x axis	$0.0006^\circ$	$0.0007^\circ$
2.5	Rotation of reflector around y axis	$0.0006^\circ$	$0.0007^\circ$
2.6	Rotation of reflector around z axis	$0.001^\circ$	$0.0006^\circ$

Table 4: Gravitation/temperature stability tolerances for reflector.

In Table 5 the maximum deformations of the whole antenna are listed and compared with the TICRA requirements in the global coordinate system. These deformations are found from averaging deformations and rotations of the two upper reflector corners and feed horn 4 center point relative to the origin of the global coordinate system. The rotation in 3.4 slightly exceeds the requirement, but is deemed acceptable.

		TICRA analysis	FEM results max deformation
3.1	Movement of frf in x direction	$\pm 10 \mu\text{m}$	$4.3 \mu\text{m}$
3.2	Movement of frf in y direction	$\pm 15 \mu\text{m}$	$4.2 \mu\text{m}$
3.3	Movement of frf in z direction	$\pm 5 \mu\text{m}$	$2.6 \mu\text{m}$
3.4	Rotation of frf around x axis	$\pm 0.0012^\circ$	$0.0014^\circ$
3.5	Rotation of frf around y axis	$\pm 0.0012^\circ$	$0.0007^\circ$
3.6	Rotation of frf around z axis	$\pm 0.003^\circ$	$0.0005^\circ$

Table 5: Gravitation/temperature stability tolerances for feed cluster+reflector+frame (frf).

## 6 CONCLUSIONS

A new specially designed antenna to be used for inter-comparisons and validation of antenna test facilities is under development in cooperation between DTU and TICRA under a contract from the European Space Agency.

The antenna is designed to be extremely thermally and mechanically stable in the temperature range  $20 \pm 5^\circ\text{C}$  and under arbitrary orientation in the gravity field. It is shown by FEA that the CFRP support frame and reflector with Invar36 fittings is able to meet the acceptable deformations found by electromagnetic analyses. A solution to integrate the aluminum feed cluster with high thermal expansion coefficient into the CFRP support frame with low thermal expansion coefficient, without compromising the acceptable deformations, is also presented.

## ACKNOWLEDGEMENTS

This work is supported and performed under ESA contract 4000109866/13/NL/MH “Millimeter wave Validation Standard (mm-VAST) antenna”.

## REFERENCES

- [1] DTU-ESA Spherical Near-Field Antenna Test Facility. Homepage, [http://www.ems.elektro.dtu.dk/research/dtu\\_esa\\_facility](http://www.ems.elektro.dtu.dk/research/dtu_esa_facility).
- [2] S. Pivnenko et al, Comparison of Antenna Measurement Facilities With the DTU-ESA 12 GHz Validation Standard Antenna Within the EU Antenna Centre of Excellence. *IEEE Trans. Ant. Propagat.*, vol. 57, no. 7, pp. 1863–1878, 2009.
- [3] S. Pivnenko, O.S. Kim, O. Breinbjerg, K. Branner, C.M. Markussen, R. Jørgensen, N.V. Larsen and M. Paquay, DTU-ESA millimeter-wave validation standard antenna – Requirements and design. *Proceedings of the 36th Annual Symposium of the Antenna Measurement Techniques Association (AMTA)*. IEEE, Tucson, Arizona, USA, 2014.
- [4] O.S. Kim, S. Pivnenko, O. Breinbjerg, K. Branner, P. Berring, C.M. Markussen, R. Jørgensen, N.V. Larsen and M. Paquay, DTU-ESA millimeter-wave validation standard antenna (mm-VAST) – Detailed design. *Proceedings of the 9th European Conference on Antennas and Propagation (EuCAP'2015)*, Lisbon, Portugal, 12-17 April 2015.